SCIENCE CHINA Information Sciences



• LETTER •

January 2026, Vol. 69, Iss. 1, 119403:1–119403:2 https://doi.org/10.1007/s11432-025-4506-1

$32 \times 32 \beta$ -Ga₂O₃ MOS solar-blind ultraviolet detector array and its properties

Haifeng CHEN^{1*}, Chenlu WU¹, Xuyang LIU¹, Chunling CHEN¹, Huorong WANG², Qin LU¹, Xiangtai LIU¹, Jinyu NI³, Zhan WANG¹ & Shaoqing WANG¹

¹Key Laboratory of Advanced Semiconductor Devices and Materials, School of Electronic Engineering, Xi'an University of Posts and Telecommunications, Xi'an 710121, China

²Xi'an Nova StarTech Co., Ltd., Xi'an 710061, China

³China Nanhu Academy of Electronics and Information Technology, Jiaxing 314000, China

Received 1 April 2025/Revised 5 May 2025/Accepted 18 June 2025/Published online 22 September 2025

Citation Chen H F, Wu C L, Liu X Y, et al. 32×32 β -Ga₂O₃ MOS solar-blind ultraviolet detector array and its properties. Sci China Inf Sci, 2026, 69(1): 119403, https://doi.org/10.1007/s11432-025-4506-1

Ga₂O₃ has an ultra-wide bandgap of 4.5-5.3 eV and is an ideal solar-blind ultraviolet (SUV) detection material [1]. With the surge in demand for image sensors with different wavelength sensing capabilities for machine vision applications based on artificial intelligence, Ga₂O₃ SUV detection has begun to expand from a single detector to a multi detector imaging array [2]. At present, most studies on Ga₂O₃ array detectors are based on a metalsemiconductor-metal (MSM) structure. However, this relatively simple structure is susceptible to the persistent photoconductivity (PPC) effect because it lacks an active switching function during the illumination process. In 2023, Zhang et al. [3] prepared a Sigate Ga₂O₃ field effect transistor (FET) photodetector. Based on the dynamic alternating gate voltage modulation, the PPC effect was well suppressed, which offers a useful attempt to construct a high-performance FET photodetector. Similar to the Si-gate FET, the metal oxide semiconductor (MOS) FET suppresses PPC via gate control. Compared with the Si-gate FET, the MOSFET is easier to integrate into large-scale arrays. Nonetheless, some problems remain unsolved with regard to the preparation process and physical characteristics. As a result, the progress of large-scale Ga₂O₃ MOSFET detector arrays has been slow. In this study, a 32 \times 32 β -Ga₂O₃ MOSFET SUV detector array was prepared. The photoelectric characteristics, gate-controlled reset function, and imaging performance of the array were analyzed in detail, and the relevant physical mechanism was determined.

Experiment. The prepared 32 \times 32 MOSFET detector array is shown in Figure 1(a). The array size is 7 mm \times 7 mm. Figure 1(b) shows the equivalent circuit diagram of the array with row and column wires. The upper part of Figure 1(c) is a locally enlarged view of the array. The lower part of Figure 1(c) shows the size of a single pixel unit (170 μ m \times 200 μ m) and other dimension parameters. During exposure, the source is grounded, and the pixel to be illuminated is selected by applying gate bias V_G (to select the column) and the drain bias V_D (to select the row). The specific preparation process of the array is detailed in Appendix A.

Results and discussion. Figure 1(d) shows the classic output curve of the MOSFET under darkness. The drain current I_D is very small on the nanoampere scale, even at $V_G=5$ V. Under the SUV irradiation with an intensity (P) of 1250 μ W/cm², as shown in Figure 1(e), I_D increases greatly. This increase is attributed to the ample photo-generated electrons in the Ga₂O₃ film; the enhanced I_D is on the μ A scale. Figure 1(f) shows the variations in the photo-dark current ratio (PDCR) under different V_G and V_D . The optimal PDCR point corresponds to $V_G=2$ V/ $V_D=2$ V and is about 3×10^3 . As seen from Figure 1(g), the device in this bias case exhibits good time response characteristics, and its rise time τ_r and decay time τ_d are only 62 and 89 ms, respectively.

In Figure 1(h), I_D at $\,V_G=2$ V is approximately 1.22 $\,\mu\mathrm{A}$ under SUV light of 1250 $\mu W/cm^2$. It changes to 1×10^{-8} A after turning off the SUV light for 4 s. Obviously, I_D cannot be restored to its initial dark current value of about 4×10^{-10} A because of the PPC effect. The negative V_G drives away the electrons in the channel and suppresses the PPC. The inset in Figure 1(h) shows that the dark current at $V_G = -10$ V is ultra-low; thus, the device demonstrates the excellent capability to suppress the photo current of $V_G = 2$ V. After applying $V_G = -10$ V for 4 s in the next light on-off cycle, the photo current of $V_G = 2$ V is effectively attenuated to the minimum value of approximately 1.58 pA, as shown in Figure 1(h). Therefore, the current suppression ratio is very large and reaches up to about 7.7×10^5 . This experimental result implies that resetting $V_G = -10$ V effectively suppresses the PPC effect. Further, Figure 1(i) shows the switching process of gate modulation under continuous SUV light irradiation of 1250 μW/cm². The upper part of Figure 1(i) shows the measurement setup. A load resistor (1 M Ω) is connected in series with the drain of the device, and then connected to the supply voltage (VDD = 5 V). The source terminal of the MOSFET is grounded, and a square wave pulse is applied to the gate (high level: $V_G =$ 2 V; low level: $V_G = -10$ V; and frequency: 1 kHz). I_D generates a voltage drop across the load resistor, thereby causing voltage division. The variation in the drain voltage (V_{out}) with a square

 $[\]hbox{* Corresponding author (email: chenhaifeng@xupt.edu.cn)}\\$

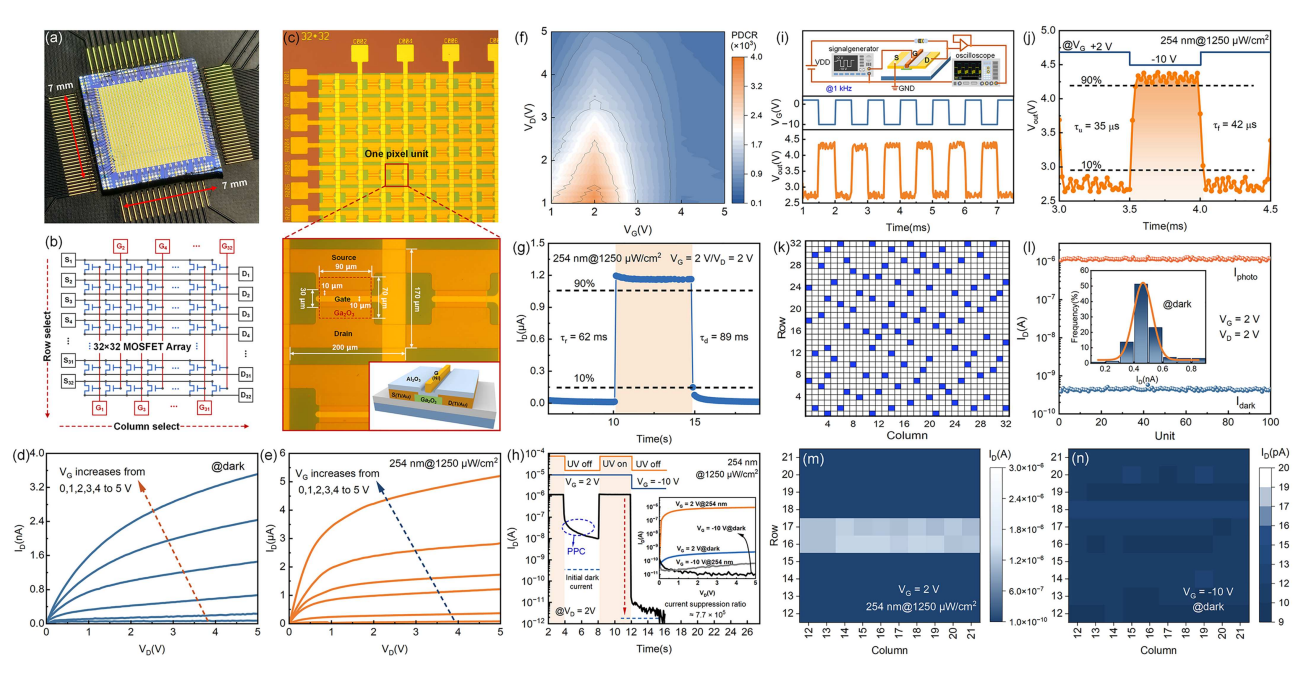


Figure 1 (Color online) (a) Image of the prepared 32 × 32 metal oxide semiconductor field effect transistor (MOSFET) array; (b) equivalent circuit of the array; (c) local magnification diagram and micrograph of a single pixel; experimental I_D - V_D curves of the MOSFET under (d) darkness and (e) 254 nm solar-blind ultraviolet (SUV) irradiation; (f) distribution of the photo-dark current ratio (PDCR) under different V_G and V_D ; (g) time response of the device; (h) I_D suppression effect of the applied negative V_G (-10 V) (the inset shows the I_D curves for $V_G=2 \text{ V}$ vs. $V_G=-10 \text{ V}$ under the dark and SUV conditions); (i) V_{out} measured as a function of the applied 1 kHz V_G square wave pulses under continuous SUV illumination; (j) gate-controlled response time; (k) distribution of 100 sampling pixels in the array; (l) photo current and dark current of the array sampling points at $V_G = 2 \text{ V/V}_D =$ 2 V (the inset shows the Gaussian distribution of the dark current); (m) partial 10×10 imaging results when $V_G = 2 \text{ V}/V_D = 2 \text{ V}$ and P is 1250 $\mu \text{W/cm}^2$; (n) current uniformity of the array at $V_G = -10 \text{ V/V}_D = 2 \text{ V}$.

wave pulse can be measured by an oscilloscope. This variation reflects the change in I_D and the gate-control capability. As shown in the lower part of Figure 1(i), I_D flows through the load resistor to generate a voltage drop when V_G is at a high level, and the drain voltage V_{out} is low (approximately 2.66 V). Conversely, when V_G is at the low level, the device is turned off, and V_{out} reaches a high value of 4.38 V. These experimental results show that the gate-control switching of the device is effective even at 1 kHz. To understand the gate-control response speed of the device, the rise time τ_u and fall time τ_f of the device under a single V_G square wave pulse are shown in Figure 1(j). The rise and fall times are as low as 35 and 42 µs, respectively. Thus, the device exhibits excellent switching characteristics.

Figure 1(k) shows the dark and photo current data of 100 samples distributed evenly in the array to evaluate the uniformity of device performance of the entire array. The evaluation result is shown in Figure 1(1). When $V_D = 2 \text{ V}/V_G = 2 \text{ V}$, I_D is as low as $0.4~\mathrm{nA}$ under dark conditions. It reaches $1.2~\mu\mathrm{A}$ under a $254~\mathrm{nm}$ SUV light of 1250 μW/cm². The inset of Figure 1(1) shows the distribution of dark currents using Gaussian distribution statistics and indicates that the pixels in the array exhibit good uniformity. When the 254 nm SUV beam illuminates a 0.4-mm-wide strip spot pattern on the array through a mask, the I_D of each pixel is measured under $V_G = 2 \text{ V}/V_D = 2 \text{ V}$. The partial 10×10 current output image of whole array is obtained, as shown in Figure 1(m). The device exhibits a remarkable response under spot illumination. When a negative V_G (-10 V) is applied, all the pixels are switched off, and I_D is quickly suppressed to several picoamperes, as shown in Figure 1(n). This result indicates that the array has a good reset function.

Conclusion. A $32 \times 32 \beta$ -Ga₂O₃ MOSFET SUV detector array was fabricated. For $V_G = 2 \text{ V}/V_D = 2 \text{ V}$, the PDCR of the device reached an optimal value of 3×10^3 , and its τ_r and τ_d were 62 and 89 ms, respectively. For $V_G = -10$ V, the current suppression ratio of the device increased to 7.7×10^5 . Under a 1 kHz gate square wave pulse, the gate-controlled reset response times decreased to the microsecond range ($\tau_u = 32~\mu\text{s},~\tau_f = 45~\mu\text{s}$). An imaging system was constructed to evaluate the array performance. Using this system, clear imaging results were obtained under SUV illumination. This work is expected to be helpful for advancing the development of $\mathrm{Ga_2O_3}$ MOSFET SUV image sensors.

Acknowledgements This work was supported by Natural Science Basic Research Program of Shanxi Province of China (Grant No. 2023-JC-YB-574) and National Natural Science Foundation of China (Grant No. 62304178).

Supporting information Appendixes A-C. The supporting information is available online at info.scichina.com and link.springer.com. The supporting materials are published as submitted, without typesetting or editing. The responsibility for scientific accuracy and content remains entirely with the authors.

References

- Dong L, Yu J, Jia R, et al. Self-powered MSM deep-ultraviolet β- $G_{a_2}O_3$ photodetector realized by an asymmetrical pair of Schottky contacts. Opt Mater Express, 2019, 9: 1191 Kuang S, Yang Z, Xu X, et al. Highly sensitive solar-blind ultraviolet photodetectors and 64×64 photodetector arrays realized
- by molecule beam epitaxy grown Ga₂O₃ epitaxial thin films. Adv
- by indectine beam epinaxy grown Ga_2O_3 epinaxia thin hims. Adv Opt Mater, 2025, 13: 2403049 Zhang Z F, Tan P J, Hou X H, et al. Breaking the responsivity-speed dilemma of α -GaO_x photodetector by alternating gate modulation. Sci China Inf Sci, 2023, 66: 229408